NIH Public Access
Author Manuscript
Int J Radiat Oncol Biol Phys. Author manuscript; available in PMC 2011 October 1.

Published in final edited form as:
Int J Radiat Oncol Biol Phys. 2010 October 1; 78(2): 547–554. doi:10.1016/j.ijrobp.2010.03.037.

PROTEOMIC ANALYSIS OF RADIATION-INDUCED CHANGES IN RAT LUNG: MODULATION BY THE SUPEROXIDE DISMUTASE MIMETIC, MNTE-2-PYP^{5+}

Vasily A. Yakovlev, M.D., Ph.D.[*], **Christopher S. Rabender, B.S.**[†], **Heidi Sankala, Ph.D.**[*], **Ben Gauter-Fleckenstein, M.D.**[‖,‡], **Katharina Fleckenstein, M.D.**[‖,§], **Ines Batinic-Haberle, Ph.D.**[‖], **Isabel Jackson, B.S.**[‖], **Zeljko Vujaskovic, M.D. Ph.D.**[‖], **Mitchell S. Anscher, M.D.**[*], **Ross B. Mikkelsen, Ph.D.**[*], and **Paul R. Graves, Ph.D.**[*]

[*]Department of Radiation Oncology, Virginia Commonwealth University, Richmond, VA

[†]Department of Pharmacology, Virginia Commonwealth University, Richmond, VA

[‡]Department of Anesthesiology and Intensive Care Medicine, Mannheim Medical Center, Heidelberg University, Mannheim, Germany

[§]Department of Radiation Oncology, Mannheim Medical Center, University of Heidelberg, Mannheim, Germany

[‖]Department of Radiation Oncology, Duke University Medical Center, Durham, NC.

Abstract

Purpose—To identify temporal changes in protein expression in the irradiated rat lung and generate putative mechanisms underlying the radioprotective effect of the manganese superoxide dismutase mimetic, MnTE-2-PyP^{5+}.

Methods and Materials—Female Fischer 344 rats were irradiated to the right hemithorax with a single dose of 28 Gy and euthanized from day 1 to 20 weeks after irradiation. Proteomic profiling was performed to identify proteins that underwent significant changes in abundance. Some irradiated rats were administered MnTE-2-PyP^{5+} and changes in protein expression and phosphorylation determined at 6 weeks post irradiation.

Results—Radiation induced a biphasic stress response in the lung as shown by the induction of heme oxygenase 1 at 1-3 days and at 6-8 weeks post-irradiation. At 6-8 weeks post-irradiation, the down regulation of proteins involved in cytoskeletal architecture (filamin A and talin), antioxidant defense (biliverdin reductase and peroxiredoxin II) and cell signaling (β-catenin, annexin II, and rho-GDI) was observed. Treatment with MnTE-2-PyP^{5+} partially prevented the apparent degradation of filamin and talin, reduced the level of cleaved caspases 3 and 9 and promoted Akt phosphorylation as well as β-catenin expression.

© 2010 Elsevier Inc. All rights reserved.

Address correspondence to: Paul R. Graves, Ph.D., Department of Radiation Oncology, Virginia Commonwealth University, Goodwin Research Labs, 401 College St., Richmond, VA 23298. Tel: 804-628-1707. Fax: 804-827-0635. prgraves@vcu.edu..

Publisher's Disclaimer: This is a PDF file of an unedited manuscript that has been accepted for publication. As a service to our customers we are providing this early version of the manuscript. The manuscript will undergo copyediting, typesetting, and review of the resulting proof before it is published in its final citable form. Please note that during the production process errors may be discovered which could affect the content, and all legal disclaimers that apply to the journal pertain.

Conflicts of Interest Notification: No actual or potential conflicts of interest exist.

NIH-PA Author Manuscript
NIH-PA Author Manuscript
NIH-PA Author Manuscript

NIH-PA Author Manuscript

NIH-PA Author Manuscript

NIH-PA Author Manuscript

Conclusion—A significant down regulation of proteins and an increase in protein markers of apoptosis were observed at the onset of lung injury in the irradiated rat lung. Treatment with MnTE-2-PyP^{5+}, which has been demonstrated to reduce lung injury from radiation, reduced apparent protein degradation and apoptosis indicators suggesting that preservation of lung structural integrity and prevention of cell loss may underlie the radioprotective effect of this compound.

Keywords

Radiation-induced lung injury; proteomics; heme oxygenase; superoxide dismutase; inflammation

INTRODUCTION

Radiation-induced lung injury (RILI) remains a major obstacle in the treatment of a variety of thoracic cancers (1). Some of the untoward effects of pulmonary radiation include pneumonitis occurring within the first 6 months and pulmonary fibrosis at months to years post-treatment. However, the molecular mechanisms underlying its pathogenesis remain obscure.

The molecular response to radiation in the lung is not only a function of dose but also time (2). One of the earliest events is thought to be the generation of reactive oxygen (ROS) and nitrogen species (RNS) that can promote damage to DNA, proteins and lipids (3). Another possible consequence of ROS/RNS generation is the induction of pro-inflammatory cytokines. Radiation of rat (4,5) or mouse (6-8) lungs is known to induce the expression of IL-1α, IL-1β, IL-6, TNF-α, and TGFβ in a cyclical pattern. The induction of cytokine expression in the rat occurred at very early times following irradiation (within 1 hour) and was also seen at later times (up to 16 weeks) (5). In mice, after an initial induction of cytokines, a second wave of cytokine expression was reported at 4-10 weeks (6-8).

A role for oxidative stress in RILI is supported by evidence showing that increasing manganese superoxide dismutase (MnSOD) activity through the use of synthetic MnSOD mimetics (9-13) or by the introduction of MnSOD itself (14,15) reduces lung injury from radiation. The MnSOD mimetic, MnTE-2-PyP^{5+}, was shown to reduce the breathing rate, amount of lung fibrosis and levels of TGFβ, HIF-1α, VEGF, and macrophage staining in the irradiated rat lung at 16 weeks post-IR (11). One proposed mechanism by which MnSOD mimetics may act to protect normal lung tissue is the prevention of cytokine induction that occurs in response to irradiation (16).

A temporal study of the molecular, histological and physiological changes in the irradiated rat lung also suggests a role for oxidative stress in the development of RILI (2). During the early response, an increase in lung weight and hypoxia is observed along with a decrease in lung perfusion. The decrease in lung perfusion is consistent with vascular injury and loss of microvessel density reported in irradiated rat lungs (17). A secondary response occurred at 6-10 weeks and was characterized by an increase in macrophage infiltration and oxidative stress. As lung injury progresses, parenchymal cell death can stimulate myofibroblast proliferation and the development of lung fibrosis (18).

Although a number of factors have been identified to play a role in RILI, other undiscovered factors or processes may also be involved. Therefore, to gain further insight into the underlying mechanisms of lung injury from radiation and determine how MnSOD mimetics function to reduce lung injury, we performed a proteomic analysis on irradiated rat lung tissue collected from a previously published study (2).

NIH-PA Author Manuscript

NIH-PA Author Manuscript

NIH-PA Author Manuscript

METHODS AND MATERIALS

Animals and irradiation

All rats were housed, irradiated, and euthanized at Duke University with prior approval from the Institutional Animal Care and Use Committee of Duke University (Durham, NC). Female Fischer-344 rats, aged 10-12 weeks, were housed three per cage and food and water were provided *ad libitum*. The animals were anesthetized before irradiation with an intraperitoneal injection of ketamine (65 mg/kg) and xylazine (4.5 mg/kg) and placed in a prone position. Hemithoracic radiation was delivered to the right lung with a single dose of 28 Gy as previously described (2). A total of 5 rats were euthanized at each time point before and at 1, 3, and 7 days, and 2, 4, 6, 8, 10, 14, and 20 weeks after irradiation for immunohistochemistry and histopathology studies as reported by Fleckenstein et al (2). Lung tissue samples were harvested for each time point and analyzed in this study. Because mass spectrometry is generally not quantitative, the initial proteomic analysis was conducted with a single animal per time point. The mass spectrometry data were confirmed in two additional sets of animals by Western blotting so that a total of 3 animals were analyzed for each time point.

Administration of MnSOD mimetic

MnTE-2-PyP^{5+} was administered to control or irradiated rats at a dose of 6 mg/kg/24h, delivered subcutaneously by osmotic pumps (Alzet® Model 2ML2, Durect Corporation, Cupertino, CA) at a dose rate of 5.0 μL/h for 14 days starting two hours after irradiation. Irradiated and non-irradiated control animals received an equivalent volume of PBS. Three animals were utilized in each of the following groups: control animals, MnTE-2-PyP^{5+} only, radiation only, and radiation with MnTE-2-PyP^{5+}.

Tissue homogenization

Rat lungs were excised and immediately snap frozen in liquid nitrogen. Frozen rat lungs were weighed and pulverized using a ratio of 20 mL of ice-cold RIPA lysis buffer/g of tissue. RIPA lysis buffer: 50 mM Tris-HCl, pH 7.5, 150 mM NaCl, 5 mM EDTA, 1% Triton X-100, 1% sodium deoxycholate, 0.1% SDS, and a 1X concentration of the HALT protease and protein phosphatase inhibitor cocktail (Pierce). Following homogenization, samples were centrifuged at 13,000 × g and supernatants recovered. Protein assays were performed using a BCA protein assay and equal amounts of protein used for SDS-PAGE and Western blotting.

Antibodies, immunoprecipitation and Western blotting

Antibodies included: HO-1 (Stressgen; SPA-895), eNOS (BD Transduction Laboratories; 610296), MnSOD (Chemicon International; MAB4081), and biliverdin reductase **(**Gene Tex; 19260**)**. Antibodies to actin (sc-1615), filamin A (sc-17749), talin (sc-H-300), annexin II (sc-9061), Rho-GDI (sc-360), peroxiredoxin II (sc-33571), and xanthine oxidase (sc-20991), were from Santa Cruz Biotechnology. Antibodies to caspase 3 (9662), caspase 9 (9508), Akt (2967), phospho-Akt (9271S), and β-catenin (9587) were from Cell Signaling. Secondary antibodies were IRDye800-conjugated rabbit anti-IgG antibody (Rockland), Alexa Fluor® 680-conjugated goat anti-mouse IgG antibody (Molecular Probes) and Alexa Fluor® 680-conjugated rabbit anti-goat IgG antibody (Invitrogen) respectively. Fluorescence was visualized using the Odyssey Infrared Imaging System (Li-Cor Biosciences).

SDS-PAGE, silver staining and Mass spectrometry

Proteins were resolved using 8 or 12% 1-D SDS-PAGE and visualized by silver staining and protein bands excised, destained, and in-gel digested with trypsin as previously described (19). Protein identification was performed using an Applied Biosystems QSTAR® pulsar XL mass spectrometer as previously described (19).

NIH-PA Author Manuscript

NIH-PA Author Manuscript

NIH-PA Author Manuscript

Statistical analysis

All data are presented as mean +/- standard error of the mean. Non-irradiated controls were compared to each condition using one-way ANOVA followed by a post-hoc test. P-values <0.05 indicated statistical significance.

RESULTS

To better understand the molecular mechanisms underlying RILI, we analyzed irradiated lung samples from a previously conducted study (2) for temporal changes in protein levels. Total lung cell lysates were prepared from each time point after radiation, resolved by SDS-PAGE, and proteins visualized by silver staining. Proteins that were observed to change in abundance were excised and identified by mass spectrometry (Fig. 1A and Table 1). The proteins identified are involved in cytoskeletal organization, antioxidant defense and signal transduction (Table 1). Validation of the mass spectrometry data was performed by Western analysis against the target proteins (Fig. 1B and C) unless the protein was readily observed by silver staining (e.g. hemoglobin) or in those cases where commercial antibodies were not available.

Radiation was shown to decrease lung perfusion in rats as soon as 3 days after radiation (2). In agreement with these data, we observed a steady decline in hemoglobin levels in lung homogenates with the greatest decrease observed between 2 and 4 weeks post-irradiation (Fig. 1A). However, the most conspicuous changes in protein abundance commenced at ~6 to 8 weeks post-radiation and continued until the end of the experiment at 20 weeks. During this time, several proteins including filamin, talin, annexin II, biliverdin reductase, rho-GDI, and peroxiredoxin II exhibited a dramatic decline in abundance. In the case of annexin II, at 10 weeks post-irradiation, a lower molecular weight species was detected that reacted with the annexin II antibody suggesting generation of a proteolytic fragment. In contrast, proteins such as MnSOD, xanthine oxidase and actin remained constant in abundance throughout the entire time course indicating that the protein changes observed were not due to non-specific protein degradation. Although protein levels remained constant, the activities of MnSOD and xanthine oxidase were not determined and therefore their enzymatic contribution to protection from radiation damage remains to be explored (Fig. 1 B and C).

Previous studies indicated that irradiation induces mRNA for the stress response enzyme, HO-1 in various tissues (20,21). Therefore, we examined irradiated rat lungs over the period from one day to 20 weeks post-irradiation for HO-1 protein expression as one indicator of cellular stress. We observed a significant increase in HO-1 protein expression at 1-3 days and again at 6-8 weeks post-irradiation suggesting the appearance of a secondary inflammatory response (Fig. 2). The second induction of HO-1 was also transient and was not maintained for the entire time course. Because of the potential contribution of Wnt signaling in fibrosis (22) we also analyzed the protein levels of β-catenin in the irradiated rat lung. The protein level of β-catenin exhibited a significant decline commencing at ~4-6 weeks post-irradiation and remained diminished throughout the rest of the time course (Fig. 2).

To test the role of irradiation-induced oxidative stress in regulating protein levels in the lung, we administered rats MNTE-2-PYP^{5+} continuously for the first two weeks after radiation. This regimen was chosen based upon a previous study that showed an identical treatment schedule with MNTE-2-PYP^{5+} mitigated lung injury in rats treated with 28 Gy (11). MNTE-2-PYP^{5+} treatment decreased breathing rate, lung fibrosis, and staining of 8-OHdG, TGF-β, HIF-1α, VEGF, and CA-IX in the lung at 16 weeks post-IR (11). We analyzed how treatment with the MnSOD mimetic altered protein levels at 6 weeks post-IR, a time chosen because it corresponds to macrophage infiltration into the lung and because it is at the cusp of a large increase in oxidative stress as shown by 8-OHdG staining (2). We found that administration of the MnSOD mimetic had no significant effect on HO-1 protein expression, suggesting that radiation-

NIH-PA Author Manuscript

NIH-PA Author Manuscript

NIH-PA Author Manuscript

induced cell stress was not completely eliminated by this treatment (Fig. 3A, B). However, MnTE-2-PyP^{5+} significantly increased the level of phosphorylated Akt, the level of β-catenin, and decreased the apparent degradation of filamin, and cleaved caspase 3 (Fig. 3B) compared to radiation alone (Fig. 3A, B). The effect of the MnSOD mimetic was not due to a non-specific affect on protein expression as shown by similar levels of eNOS protein after treatment with MnTE-2-PyP^{5+}.

DISCUSSION

Although many factors have been identified to contribute to RILI, evidence suggests that additional undiscovered processes are involved. Therefore, we utilized mass spectrometry to identify proteins that changed in abundance in the irradiated rat lung over a time course from one day to 20 weeks post-irradiation. The lung samples were obtained from a previous study that documented physiological and histological changes after radiation (2) permitting functional correlations between protein levels and physiological outcomes. From silver staining of total lung homogenates, it was clear that the abundance of several proteins dramatically decreased between 6 and 20 weeks post-irradiation (Fig. 1A). Although it was not possible to identify all of the down-regulated proteins due to the complex nature of the samples, the most prominent proteins were identified. These proteins are involved in processes ranging from cellular architecture to cell signaling (Table 1) and have not yet been reported to undergo radiation-induced changes in the lung. One protein that underwent a dramatic change is filamin, whose protein level dropped precipitously at 6 weeks post-IR and remained low throughout the remainder of the time course. Filamin is a large scaffolding protein involved in cross-linking actin filaments and organization of the cytoskeleton (23). Interestingly, filamin-A knock-out mice show vascular defects with abnormal epithelial and endothelial organization and aberrant adherens junctions in developing blood vessels (24). Thus, loss of filamin A may contribute to vascular damage and subsequent hypoxia in the lung. Another protein identified to be down regulated was talin which plays a critical role in integrin activation and actin cytoskeleton dynamics (25).

Other proteins down-regulated between 8 and 20 weeks post-IR were biliverdin reductase and peroxiredoxin II. Both biliverdin reductase and peroxiredoxin II contribute to antioxidant defense by production of bilirubin (26) and reduction of hydrogen peroxide to water respectively. The decrease in the level of these enzymes correlates with a steep increase in oxidative stress in rat lungs as measured by 8-OHdG staining between 6 and 10 weeks post-radiation (2). Thus, loss of biliverdin reductase and peroxiredoxin II may be one mechanism by which radiation contributes to establishment of chronic oxidative stress. In agreement with our results, biliverdin reductase and peroxiredoxin II were previously shown to be down regulated in abundance in mouse lungs 5 weeks after treatment with 12 Gy (27).

In addition to the proteins mentioned above, we found that Rho-GDI and annexin II were down regulated in abundance. Rho-GDI inhibits GDP dissociation from Rho GTPases, keeping the latter in an inactive state (28). The Rho GTPases are involved in the regulation of a diverse array of cellular processes including actin dynamics, gene transcription, and motility (29). Thus, alteration of their activity could potentially impact a large number of processes in the lung including cell migration. Annexin II was shown to undergo a dramatic reduction in apparent molecular weight at 10 weeks post-irradiation. Since the newly generated species reacted with the annexin II antibody, one possibility is limited proteolysis. Annexin II has been shown to be cleaved by proteases into a 33 kDa C-terminal core domain and a 3 kDa N-terminal domain of 30 amino acids (30) and Annexin II forms in the 32-36 kDa range were identified by mass spectrometry (31). Interestingly, antibodies to annexin were detected in the sera and bronchoalveolar lavage fluid from patients with idiopathic pulmonary fibrosis (32).

NIH-PA Author Manuscript

NIH-PA Author Manuscript

NIH-PA Author Manuscript

In contrast to the proteins identified by mass spectrometry, we found that the HO-1 expression was upregulated by radiation. HO-1 is a low molecular weight stress protein that catalyzes the oxidative degradation of heme to biliverdin, carbon monoxide and iron and is induced by a wide variety of stress signals (26). Previous studies of HO-1 and radiation have shown increases in HO-1 in response to ionizing radiation in rat liver (33), intestine (34) and mouse lung (20, 21). However, the studies of mouse lung only showed mRNA changes for HO-1 (20,21). We have shown for the first time that HO-1 protein expression is increased after irradiation of the lung and that in addition to the first induction, a second induction of HO-1 protein expression occurs at 6-8 weeks post-irradiation suggesting the onset of a second wave of cellular stress.

Previous studies have shown that MnSOD mimetics have the ability to reduce RILI in animal models (9-13). Although they are capable of reducing RILI, the mechanisms underlying their protective effects are not fully elucidated. Therefore, we analyzed protein expression changes in the irradiated rat lung from animals treated with the MnSOD mimetic, MnTE-2-PyP^{5+} at 6 weeks post-radiation, a time corresponding to macrophage and other inflammatory cell infiltration (2). Treatment of rats with MnTE-2-PyP^{5+} did not result in a reduction in the amount of HO-1 expression at 6 weeks post-IR. This result may be due to the fact that many different types of signals, other than ROS/RNS, induce HO-1 expression (26) or because MnTE-2-PyP^{5+} does not completely eliminate lung injury (2). However, MnTE-2-PyP^{5+} treatment did reduce the apparent degradation of filamin as shown by a decrease in the amount of a ~250 kDa band which reacts with the filamin antibody and was identified as filamin by mass spectrometry (Fig. 1 and Table 1, ID #3). Therefore, one mechanism of MnSOD mimetics may be to reduce levels of protein proteolysis.

β-catenin protein levels were significantly down regulated in abundance beginning at ~4-6 weeks post-irradiation and remained diminished until the end of the study (Fig. 2). MnTE-2-PyP^{5+} treatment significantly increased β-catenin protein levels at 6 weeks post-radiation compared to radiation alone (Fig. 3A and B). β-catenin is an integral part of the Wnt signaling pathway and irradiation has been shown to inhibit β-catenin signaling in epithelial cells (35). Moreover, activation of β-catenin in epithelial cells improves cell survival after irradiation (36). However, there are also studies that show that aberrant Wnt signaling may contribute to pulmonary fibrosis (22).

Treatment with MnTE-2-PyP^{5+} also increased the level of phosphorylated Akt in the irradiated rat lung. Activation of Akt in normal tissues is generally thought to promote cell survival and proliferation and exposure of normal cells to a variety of forms of stress, including ionizing radiation, reduces Akt activation (37). In agreement with these findings, we found that irradiation decreased Akt phosphorylation at 6 weeks post-IR. Therefore, the increased level of Akt phosphorylation observed after MnTE-2-PyP^{5+} treatment may reflect an increase in cell survival signaling. In support of this, treatment with MnTE-2-PyP^{5+} produced a corresponding decrease in the amount of cleaved caspase 3. This is in agreement with a previous study that found that a MnSOD mimetic reduced irradiation-induced caspase 3 activation in U937 cells (13). Taken together, these data suggest that one mechanism by which the MnSOD mimetics act to reduce RILI is to reduce the level of cell death.

In summary, we have identified novel protein changes occurring both during the early response and during the progression and development of RILI at 6-20 weeks after irradiation. It is not yet determined if the changes in protein levels are due to differential protein expression, protein turnover, or from reorganization/remodeling of lung tissue. A model summarizing a potential mechanism for the protective effects of MnSOD mimetics is shown in Fig. 4. In this model, radiation induces lung injury in part through the generation of ROS/RNS, which in turn, can induce significant protein down regulation. The loss of proteins involved in oxidative stress metabolism may further contribute to the generation of ROS/RNS. Alternatively, the loss of

NIH-PA Author Manuscript

NIH-PA Author Manuscript

NIH-PA Author Manuscript

cytoskeletal proteins could disrupt connections to the extracellular matrix and induce apoptotic processes. Increased cell death may then stimulate the recruitment of macrophages and other inflammatory cells that can further increase levels of ROS/RNS creating a cycle of chronic inflammation. To maintain structural integrity of the lung, dead cells are replaced by myofibroblasts that ultimately can contribute to the fibrotic process (18). Thus, MnSOD mimetics may function to reduce radiation-induced lung injury by interrupting the cycle of chronic inflammation through reduction of ROS/RNS and by reducing the level of protein down regulation and apoptosis to preserve structural integrity of the lung.

Acknowledgments

This research was supported by NIH grants P01 CA72955 (RBM), RO1 CA90881(RBM), U19AI067798(ZV), R01 CA 098452(ZV) and an American Heart Scientific Development Grant 0835471N (PRG).

Abbreviations

HO-1	Heme oxygenase I
MnSOD	Manganese superoxide dismutase
IR	irradiation
RILI	radiation-induced lung injury
ROS	Reactive oxygen species
RNS	reactive nitrogen species

REFERENCES

1. Abratt RP, Morgan GW. Lung toxicity following chest irradiation in patients with lung cancer. Lung Cancer 2002;35:103–109. [PubMed: 11804681]
2. Fleckenstein K, Zgonjanin L, Chen L, et al. Temporal onset of hypoxia and oxidative stress after pulmonary irradiation. Int J Radiat Oncol Biol Phys 2007;68:196–204. [PubMed: 17448873]
3. Zhao W, Robbins ME. Inflammation and chronic oxidative stress in radiation-induced late normal tissue injury: therapeutic implications. Curr Med Chem 2009;16:130–143. [PubMed: 19149566]
4. Bao P, Gao W, Li S, et al. Effect of pretreatment with high-dose ulinastatin in preventing radiation-induced pulmonary injury in rats. Eur J Pharmacol 2009;603:114–119. [PubMed: 19101537]
5. Calveley VL, Khan MA, Yeung IW, et al. Partial volume rat lung irradiation: temporal fluctuations of in-field and out-of-field DNA damage and inflammatory cytokines following irradiation. Int J Radiat Biol 2005;81:887–899. [PubMed: 16524844]
6. Rube CE, Uthe D, Schmid KW, et al. Dose-dependent induction of transforming growth factor beta (TGF-beta) in the lung tissue of fibrosis-prone mice after thoracic irradiation. Int J Radiat Oncol Biol Phys 2000;47:1033–1042. [PubMed: 10863076]
7. Rube CE, Wilfert F, Palm J, et al. Irradiation induces a biphasic expression of pro-inflammatory cytokines in the lung. Strahlenther Onkol 2004;180:442–448. [PubMed: 15241532]
8. Rubin P, Johnston CJ, Williams JP, et al. A perpetual cascade of cytokines postirradiation leads to pulmonary fibrosis. Int J Radiat Oncol Biol Phys 1995;33:99–109. [PubMed: 7642437]
9. Vujaskovic Z, Batinic-Haberle I, Rabbani ZN, et al. A small molecular weight catalytic metalloporphyrin antioxidant with superoxide dismutase (SOD) mimetic properties protects lungs from radiation-induced injury. Free Radic Biol Med 2002;33:857–863. [PubMed: 12208373]
10. Rabbani ZN, Batinic-Haberle I, Anscher MS, et al. Long-term administration of a small molecular weight catalytic metalloporphyrin antioxidant, AEOL 10150, protects lungs from radiation-induced injury. Int J Radiat Oncol Biol Phys 2007;67:573–580. [PubMed: 17236973]

NIH-PA Author Manuscript

NIH-PA Author Manuscript

NIH-PA Author Manuscript

11. Gauter-Fleckenstein B, Fleckenstein K, Owzar K, et al. Comparison of two Mn porphyrin-based mimics of superoxide dismutase in pulmonary radioprotection. Free Radic Biol Med 2008;44:982–989. [PubMed: 18082148]
12. Langan AR, Khan MA, Yeung IW, et al. Partial volume rat lung irradiation: the protective/mitigating effects of Eukarion-189, a superoxide dismutase-catalase mimetic. Radiother Oncol 2006;79:231–238. [PubMed: 16675053]
13. Lee JH, Lee YM, Park JW. Regulation of ionizing radiation-induced apoptosis by a manganese porphyrin complex. Biochem Biophys Res Commun 2005;334:298–305. [PubMed: 16002045]
14. Greenberger JS, Epperly MW, Gretton J, et al. Radioprotective gene therapy. Curr Gene Ther 2003;3:183–195. [PubMed: 12762478]
15. Epperly MW, Defilippi S, Sikora C, et al. Intratracheal injection of manganese superoxide dismutase (MnSOD) plasmid/liposomes protects normal lung but not orthotopic tumors from irradiation. Gene Ther 2000;7:1011–1018. [PubMed: 10871749]
16. Jackson IL, Chen L, Batinic-Haberle I, et al. Superoxide dismutase mimetic reduces hypoxia-induced O2*-, TGF-beta, and VEGF production by macrophages. Free Radic Res 2007;41:8–14. [PubMed: 17164174]
17. Ghosh SN, Wu Q, Mader M, et al. Vascular injury after whole thoracic x-ray irradiation in the rat. Int J Radiat Oncol Biol Phys 2009;74:192–199. [PubMed: 19362237]
18. Rodemann HP, Blaese MA. Responses of normal cells to ionizing radiation. Semin Radiat Oncol 2007;17:81–88. [PubMed: 17395038]
19. Zeng Y, Sankala H, Zhang X, et al. Phosphorylation of Argonaute 2 at serine-387 facilitates its localization to processing bodies. Biochem J 2008;413:429–436. [PubMed: 18476811]
20. Risom L, Moller P, Vogel U, et al. X-ray-induced oxidative stress: DNA damage and gene expression of HO-1, ERCC1 and OGG1 in mouse lung. Free Radic Res 2003;37:957–966. [PubMed: 14670003]
21. Han Y, Platonov AG, Akhalaia M, et al. Tissue-specific changes in heme oxygenase activity and level of nonprotein thiols in C57Bl/6 mice after whole-body gamma-irradiation. Bull Exp Biol Med 2005;140:341–344. [PubMed: 16307054]
22. Chilosi M, Poletti V, Zamo A, et al. Aberrant Wnt/beta-catenin pathway activation in idiopathic pulmonary fibrosis. Am J Pathol 2003;162:1495–1502. [PubMed: 12707032]
23. Popowicz GM, Schleicher M, Noegel AA, et al. Filamins: promiscuous organizers of the cytoskeleton. Trends Biochem Sci 2006;31:411–419. [PubMed: 16781869]
24. Feng Y, Chen MH, Moskowitz IP, et al. Filamin A (FLNA) is required for cell-cell contact in vascular development and cardiac morphogenesis. Proc Natl Acad Sci U S A 2006;103:19836–19841. [PubMed: 17172441]
25. Ziegler WH, Gingras AR, Critchley DR, et al. Integrin connections to the cytoskeleton through talin and vinculin. Biochem Soc Trans 2008;36:235–239. [PubMed: 18363566]
26. Ryter SW, Alam J, Choi AM. Heme oxygenase-1/carbon monoxide: from basic science to therapeutic applications. Physiol Rev 2006;86:583–650. [PubMed: 16601269]
27. Ao X, Lubman DM, Davis MA, et al. Comparative proteomic analysis of radiation-induced changes in mouse lung: fibrosis-sensitive and -resistant strains. Radiat Res 2008;169:417–425. [PubMed: 18363430]
28. DerMardirossian C, Bokoch GM. GDIs: central regulatory molecules in Rho GTPase activation. Trends Cell Biol 2005;15:356–363. [PubMed: 15921909]
29. Bishop AL, Hall A. Rho GTPases and their effector proteins. Biochem J 2000;348(Pt 2):241–255. [PubMed: 10816416]
30. Waisman DM. Annexin II tetramer: structure and function. Mol Cell Biochem 1995;149-150:301–322. [PubMed: 8569746]
31. Singh P. Role of Annexin-II in GI cancers: interaction with gastrins/progastrins. Cancer Lett 2007;252:19–35. [PubMed: 17188424]
32. Kurosu K, Takiguchi Y, Okada O, et al. Identification of annexin 1 as a novel autoantigen in acute exacerbation of idiopathic pulmonary fibrosis. J Immunol 2008;181:756–767. [PubMed: 18566442]
33. Suzuki K, Mori M, Kugawa F, et al. Whole-body X-irradiation induces acute and transient expression of heme oxygenase-1 in rat liver. J Radiat Res (Tokyo) 2002;43:205–210. [PubMed: 12238335]

NIH-PA Author Manuscript

NIH-PA Author Manuscript

NIH-PA Author Manuscript

34. Giris M, Erbil Y, Oztezcan S, et al. The effect of heme oxygenase-1 induction by glutamine on radiation-induced intestinal damage: the effect of heme oxygenase-1 on radiation enteritis. Am J Surg 2006;191:503–509. [PubMed: 16531144]

35. Gurung A, Uddin F, Hill RP, et al. Beta-catenin is a mediator of the response of fibroblasts to irradiation. Am J Pathol 2009;174:248–255. [PubMed: 19036807]

36. Woodward WA, Chen MS, Behbod F, et al. WNT/beta-catenin mediates radiation resistance of mouse mammary progenitor cells. Proc Natl Acad Sci U S A 2007;104:618–623. [PubMed: 17202265]

37. Zundel W, Giaccia A. Inhibition of the anti-apoptotic PI(3)K/Akt/Bad pathway by stress. Genes Dev 1998;12:1941–1946. [PubMed: 9649498]

NIH-PA Author Manuscript
NIH-PA Author Manuscript
NIH-PA Author Manuscript

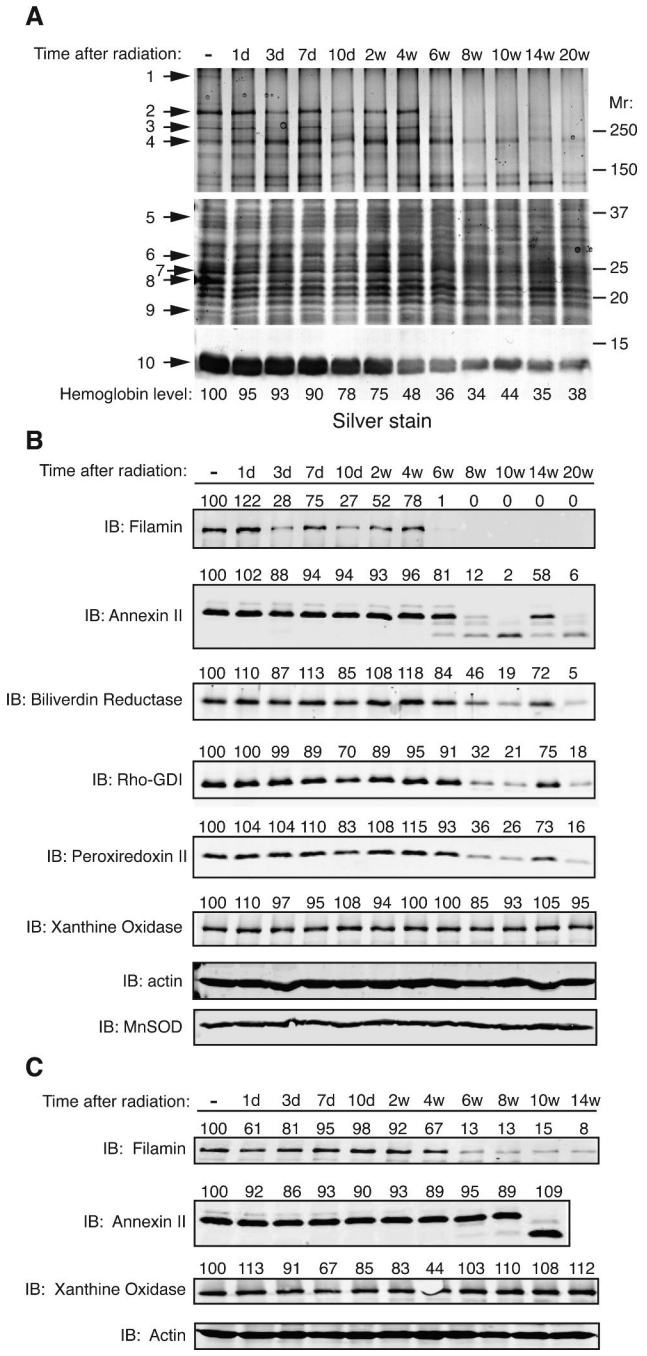

Fig. 1.

Temporal changes in protein abundance in irradiated rat lungs. (**A**) Rat lung homogenates were prepared at the indicated times after radiation, resolved by one-dimensional SDS-PAGE and proteins visualized by silver staining. Numbered arrows denote proteins that were excised and subjected to mass spectrometry with protein identity shown in Table 1. Abbreviations: "-" indicates non-irradiated control; "d" = days, "w"= weeks. The amount of hemoglobin was quantitated by densitometry, normalized to actin, and shown as a percent of the non-irradiated control. (**B**) Validation of mass spectrometry results by Western analysis. Total cell lysates from rat lung homogenates were immunoblotted with the indicated antibodies. Actin served as a loading control. (**C**) A separate group of rats were treated identically and lung tissues

NIH-PA Author Manuscript

NIH-PA Author Manuscript

NIH-PA Author Manuscript

harvested and analyzed by Western analysis. For all samples, the amount of each protein was quantitated by densitometry, normalized to actin levels, and presented as a percent of the non-irradiated control above each lane.

NIH-PA Author Manuscript
NIH-PA Author Manuscript
NIH-PA Author Manuscript

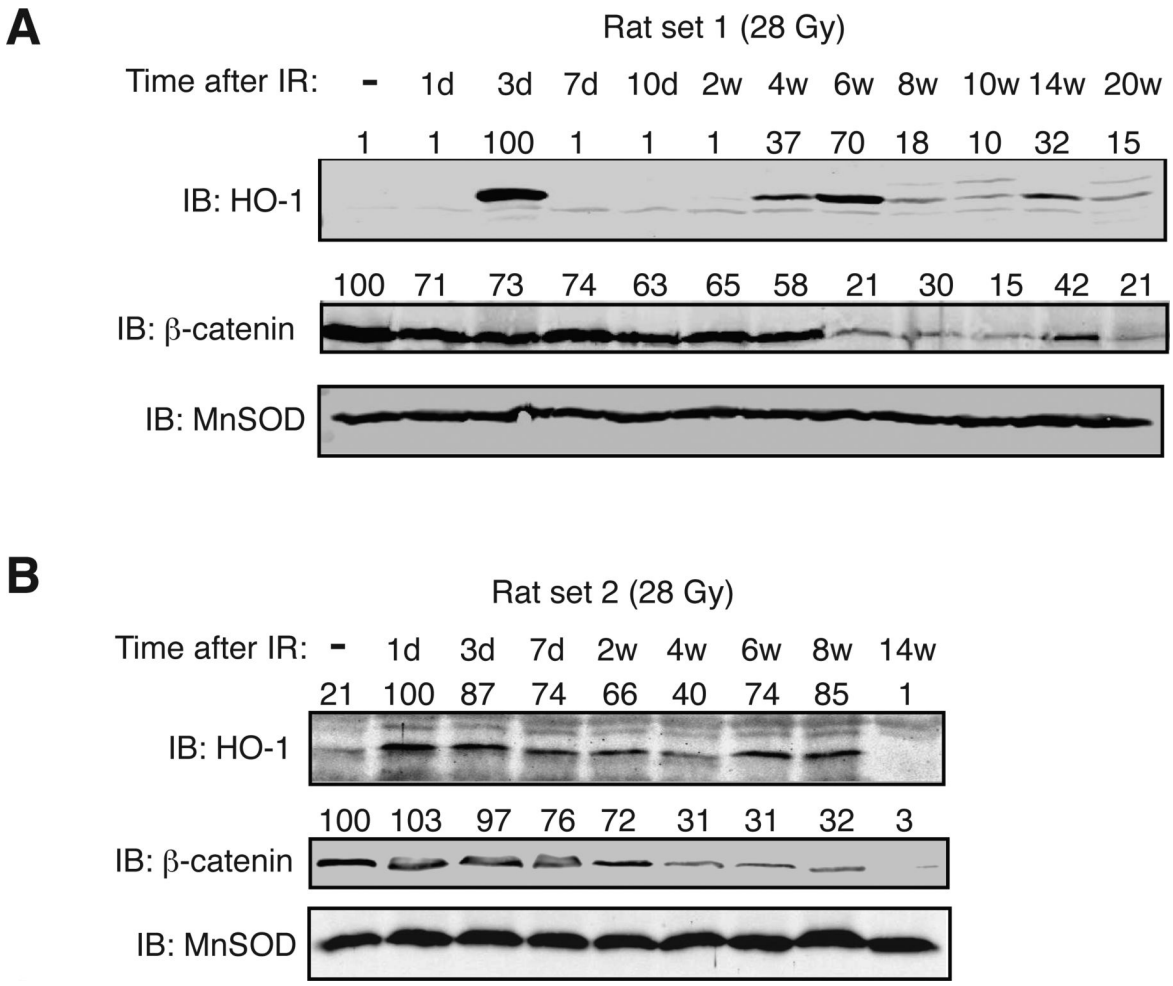

Fig. 2.

Temporal changes in Heme oxygenase 1 and β-catenin protein levels in the irradiated rat lung. (**A**) Rats were exposed to a single dose of 28 Gy to the right hemithorax and whole lung homogenates immunoblotted with HO-1 or β-catenin antibodies at the indicated times post-irradiation. Abbreviations: "-" indicates non-irradiated control; "d" = days, "w"= weeks. MnSOD served as a loading control. (**B**) A separate group of rats were treated as described in panel A. The amount of each protein was quantitated by densitometry, normalized to MnSOD levels, and presented as a percent of the non-irradiated control above each lane.

NIH-PA Author Manuscript
NIH-PA Author Manuscript
NIH-PA Author Manuscript

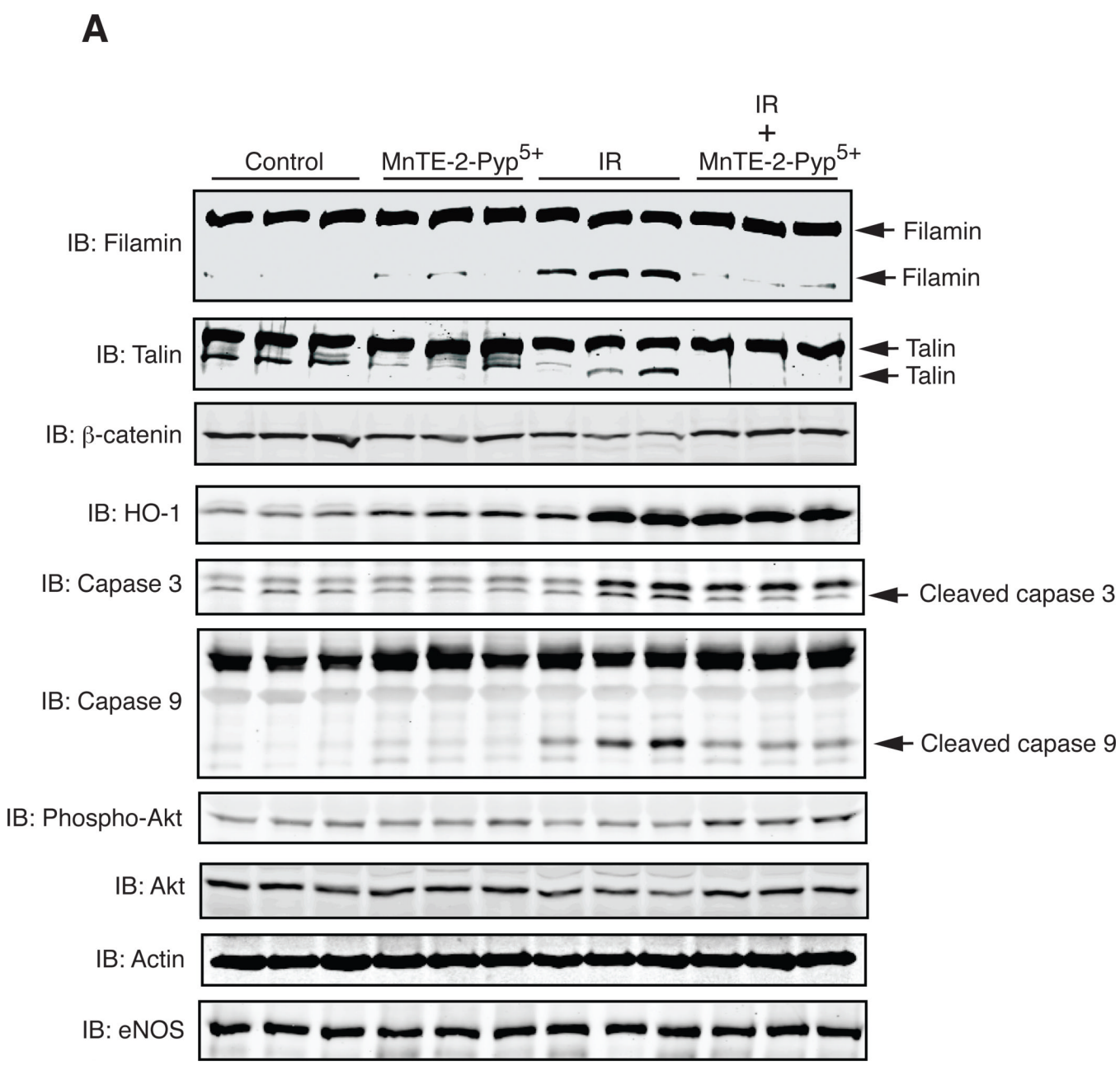

NIH-PA Author Manuscript

NIH-PA Author Manuscript

NIH-PA Author Manuscript

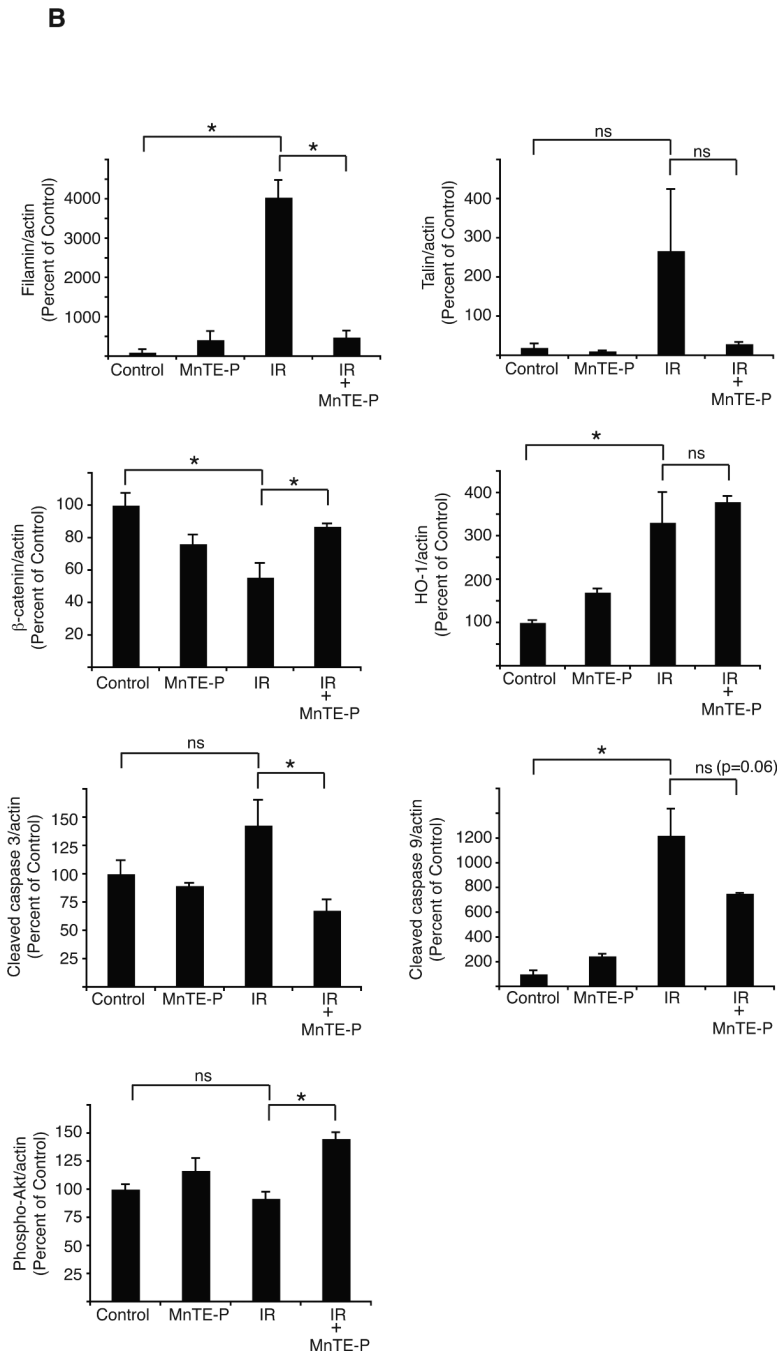

Fig. 3.

Reduction of apparent protein degradation and protein indicators of apoptosis in the irradiated lung by MnTE-2-PyP^{5+}. (**A**) Western analysis of rat lung samples prepared from 3 separate rats for each condition including: mock irradiation, irradiation alone, MnTE-2-PyP^{5+} treatment, and MnTE-2-PyP^{5+} plus irradiation at 6 weeks post-irradiation. Samples were resolved by SDS-PAGE and immunoblotted with the indicated antibodies. Actin served as a loading control. (**B**) Quantitation of the Western blot data shown in Fig. 3A. The amount of each protein was quantitated by densitometry, normalized to actin levels, and the mean presented as a percent of the non-irradiated control along with standard error. One-way

ANOVA and post-hoc tests were performed to determine significance. '*' indicates significance with a p-value <0.05. ns= not significant.

NIH-PA Author Manuscript
NIH-PA Author Manuscript
NIH-PA Author Manuscript

NIH-PA Author Manuscript

NIH-PA Author Manuscript

NIH-PA Author Manuscript

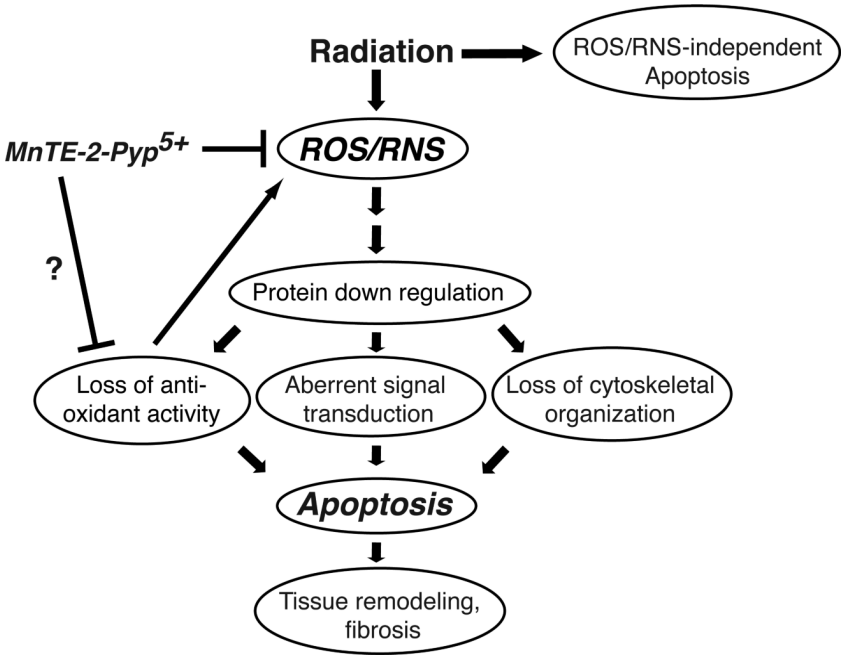

Fig. 4.

A model for the mechanism of action of MnTE-2-PyP^{5+}, in reducing lung injury from radiation. Radiation induces the generation of ROS/RNS, which in turn contributes to protein down regulation. Loss of proteins involved in ROS/RNS metabolism may contribute to further increases in ROS/RNS levels, generating a cycle of chronic inflammation. The SOD mimetic, through reduction of ROS/RNS, interrupts the cycle of chronic inflammation, reduces the level of protein down regulation and apoptosis and acts to preserve structural integrity of the lung.

NIH-PA Author Manuscript NIH-PA Author Manuscript NIH-PA Author Manuscript

Table 1

Proteins identified to change in abundance in the irradiated rat lung

Protein bands indicated in Fig. 1A were excised and identified by mass spectrometry. Protein name, function, accession numbers, mass, and Mascot scores are shown.

ID Number	Protein Name	Protein Function	Accession Number	Mass (kDa)	Mascot Score
1	AHNAK	Unknown	ABB00054	700	169
2	Filamin A	Actin binding and scaffolding protein	EDL84990	280	1406
3	Filamin A	Actin binding and scaffolding protein	EDL84990	250	956
4	Talin	Actin and Integrin interacting protein	AAI00263	161	217
5	Annexin II	Calcium regulated membrane binding protein	Q07936	38	192
6	Biliverdin Reductase	Catalyzes conversion of biliverdin to bilirubin	AAA40830	34	154
7	Carbonic Anhydrase II	Catalyzes hydration of carbon dioxide	P27139	28	99
8	Rho-GDI	Inhibits nucleotide exchange and GTP hydrolysis on Rho proteins	Q5XI73	23	292
9	Peroxiredoxin II	Hydrogen peroxide scavenging enzyme	P35704	21	168
10	Hemoglobin beta-II chain	Oxygen transport	AAH58448	15	561